Electrical Power and Energy Systems 148 (2023) 108918

Contents lists available at ScienceDirect

International Journal of Electrical Power and Energy Systems

journal homepage: www.elsevier.com/locate/ijepes

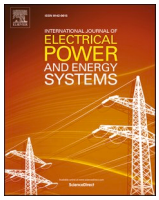

Recovery strategy of virtual power plant with resilience improvement under cascaded failure scenarios

Yue Meng, Hongli Zhang *

College of Electrical Engineering, Xinjiang University, Urumqi 830017, China

ARTICLE INFO

Keywords:
Virtual power plant (VPP)
Cascade failure
Resilience enhancement
Resilience assessment

ABSTRACT

A novel strategy resilience enhancement of using virtual power plant (VPP) systems was proposed with pre-event and post-event phases to improve plant resistance to cascading failure events. In this strategy, VPP node importance evaluation was performed based on neighbor node contributions. VPP line importance calculations were performed considering static network flows, and decision-making methods were considered for the post-disaster recovery timing scheme of the VPP system based on resilience evaluation. First, we developed the VPP system topology using complex network theory, and considered various recovery parameters of power and the information networks parameters as performance indicators. Second, a resilience index was constructed to investigate changes in the network resilience of VPP systems with recovery protocols, and the relationship between resilient recovery strategies and network recovery performance was investigated. Finally, simulations were performed on the constructed VPP system. The results of the study indicated that critical nodes and lines considerably affect network performance. The recovery strategy proposed in this study can considerably improve the post-disaster recovery ability of VPP systems and effectively address large-scale cascading failures.

1. Introduction

China, Japan, Korea, Europe, the United States of America, and other countries have incorporated carbon peaking and carbon neutrality into their development strategies [1]. A series of Internet-of-energy technologies have been integrated to scatter distributed energy resources (DERs), loads, and energy storage devices in a grid to ensure power system operation [2], enhance the efficiency of power resource utilization, and achieve energy saving and carbon reduction effects. Therefore, virtual power plants (VPPs) have attracted considerable research attention. However, energy transformation and DER development have drastically increased the operation risk of VPPs. Frequent accidents [3,4] have also exposed the vulnerability of some key types of infrastructure in coping with extreme events, and thus, highlighted the theoretical significance and application value of research to enhance the resilience of VPP systems. Resilient VPPs (RVPPs) that can effectively address all types of extreme events should be developed to ensure the long-term transformation and development of energy production and power systems.

Resilience is a measure of the ability of a system to remain stable under disturbances [5]. The term is widely used in many disciplines including power systems [6–8]. The resilience of a VPP system refers to the ability of the VPP to respond to perturbing events and the ability to prevent, defend against, and quickly restore loads for all types of extreme events. Fig. 1 illustrates the resilience properties of a VPP before, during, and after the onset of a cascade failure. The resilience promotion strategy can be categorized into two aspects: the investment strategy to ensure the safety of the system by increasing redundancy, and the operation strategy to realize the flexible operation of the system through intelligent equipment and optimization algorithm [9]. The cost of investment strategy is high but its effect is excellent. By contrast, the cost of the operation strategy is low but its effect is general. The two elasticity enhancement strategies were combined, and a novel VPP system resilience enhancement strategy that integrated pre-event reinforcement and post-event recovery was proposed.

Numerous studies have been conducted on the resilience enhancement of power systems and power information physical fusion systems. A review [10] of the current research trends in power network resilience during extreme weather events was performed from the perspective of power system engineering, and various network resilience enhancement strategies were proposed. The flexibility of the system was improved and the operational cost was reduced by scaling, location, and operation of cogeneration of a flexible electricity gas integrated microgrid system model [11]. A framework [12] was proposed for evaluating and improving the resilience of distribution network systems by formulating

* Corresponding author.

https://doi.org/10.1016/j.ijepes.2022.108918
Received 26 November 2021; Received in revised form 3 May 2022; Accepted 21 December 2022
Available online 3 January 2023

Nomenclature

Abbreviations

VPP	Virtual power plant
DER	Distributed energy resource
RVPP	Resilient virtual power plant

Main parameters and variables

i,j,l,o,d	Node label
t_{cf}	Disturbance start time
t_a	The moment when the disturbance reaches equilibrium or the whole network is paralyzed
t_r	Start rescue time
t_{drs}	The moment when the system starts to resume operation
Θ	System performance function
$LQ^C(e_{ij})$, $LQ^P(e_{ij})$	Line e_{ij} quality, where C stands for communication network and P stands for power network
$\alpha_{LOSS}(e_{ij})$	Power loss online e_{ij}
$\Phi_{e_{ij}}$	Throughput of line e_{ij}
$BW_{e_{ij}}$	Line e_{ij} bandwidth
$LCS^C(e_{ij})$,$LCS^P(e_{ij})$	Line e_{ij} significance score
Delay_L_{od}	Line delay time
γ_{od}	The number of lines passed by nodes
P_{od}	Power delivered by power node to load node
$P_L(d)$,$P_G(o)$	Load demand and generation demand
A^{-1}_{uod}	Sequential distribution matrix
NE_i	Efficiency of component i in the system
$TL(0)$	Total load of the communication network at the initial moment
V_C,V_P	Sets of information and power system nodes, respectively
k_i	degree of node i
$\tau,\alpha,t,\beta,\varphi$	Load regulating factors
LI_i,C_i,NI_i	Node load importance, Importance after optimal weighting and VPP node importance
δ	Capacity limit factor
p_i	Probability of node i failure
Ω_{ij}	Load distribution factor
Γ_i	Set of neighboring nodes of node i
Λ^t_G	Set of generator nodes recovered at time t
P^t_{Gi},Q^t_{Gi}	Active and reactive power at the generator nodes at time t
$P^{\min}_{Gi},P^{\max}_{Gi},Q^{\min}_{Gi},Q^{\min}_{Gi}$	Minimum active power, maximum active power, minimum reactive power, and maximum reactive power
V^t_j	Voltage magnitude of node j at time t
$\Delta^t_{e_{ij}}$	Line set recovered at time t
$R_{P_G},R_{P_L},R_{E_l},R_{E_V}$	Restored power supply active power, load active power, number of information flow lines, and number of VPP system transmission lines
NB_i	Component i balance
$L^C_i(0),L^P_i(0)$	Initial loads of the communication and power nodes, respectively

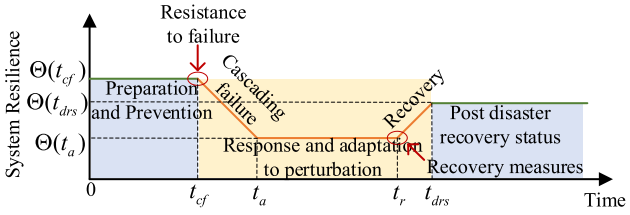

Fig. 1. Schematic of the resilience recovery process in a VPP with a cascade of failure events.

the reinforcement problem as an optimization problem and using genetic algorithms for the solution. In a study [13], mixed integer linear programming was proposed to recover priority loads for satisfying topological and operational constraints. However, the aforementioned studies cannot satisfactorily quantify resilience from the perspective of the network structure. In a study [14], a unified two-stage reconstruction method was proposed to enhance system resilience. In another study [15], a three-step analytical method was used for research on power system resilience. The use of microgrids as resilient resources was analyzed and their strategies for enhancing resilience in major power failure events was investigated. However, in [12–15], a single-layer network was the research object, which did not conform to the network property of a VPP multi-layer network. For VPP, in [16], the profits of VPP composed of demand side and factory side were based on the Shapley value to provide policy guidance for VPP promotion. In [17], the technical VPP is the scheduling unit. By selecting the optimal demand response scheme, the wind power and market price were considered uncertain parameters for power generation planning. In a study based on multi-layer network resilience [18], a novel integrated electrothermal gas model that utilized extreme historical wind and solar energy data and thermal demands were proposed to investigate the ability of a natural gas network to support a thermodynamic system with supply limitations and assess the resilience level of an integrated energy system. In a study [19], interdependent urban infrastructure system resilience based on dynamic network flow models was evaluated to quantify the resilience of distribution and subway networks to address hypothetical flood disasters. However, a VPP system is a coupled complex network that is comprised of a communication system and a power network. However, directly applying the aforementioned resilient enhancement strategies to a power system for resilience recovery and evaluation after cascade failure is difficult. Therefore, we evaluated the node and line in a VPP considering the heterogeneity of the information flow and energy flow in the VPP system and constructed a novel resilience enhancement strategy during cascade failure events that match the characteristics of the VPP system.

Hardening strategies in a virtual power plant involves changing the infrastructure to improve resilience in case of extreme natural disasters, man-made attacks, and other disruptive events. In addition to reinforcement solutions for critical nodes and lines, investigators have assessed the following strategies: (1) Use of underground transmission lines. Underground lines are well protected from the effects of extreme weather, such as hurricanes, rainstorms, ice storms, and floods on energy transmission. An underground natural gas pipelines was used [20] to replace some power transmission lines to address various extreme events and improve system resilience. (2) Emergency facilities. In this strategy, an adequate number of emergency generators, black start units, and a back-up coordination and control center were used for communication systems before the occurrence of disaster. The optimal allocation of emergency generator sets is discussed in [21], in which the effect of emergency generator reliability on energy was investigated in the case of network outage. (3) Installing guy wires and upgrading crossarm materials to strengthen towers [22], substation lifting [23], and maintaining vegetation near overhead lines [24]. Climate change and other extreme events could cause the VPP prediction to deviate from actual values. Therefore, understanding the physical mechanism of a fault to establish a simulation model is critical to copy the fault occurrence and system response and determine an appropriate preparation and reinforcement program.

The complexity of the interaction mechanisms of the virtual power plant networks is determined by the characteristics of their deep coupling. Therefore, developing an evaluation index of the node and line importance in a VPP and the resilience after recovery is typically a multi-index comprehensive evaluation problem. The optimal combinatorial empowerment method is objective, accurate, and effective in solving the decision-making problems of multi-attribute indicators. This method has been adopted in many fields, such as road transportation [25], safety risks [26], and power systems [27]. In this study, the optimal empowerment method was used to optimally empower nodes and line importance indicators as well as resilience evaluation indicators so that the indicators of various properties can be integrated to improve the VPP resilience enhancement strategy.

We investigated VPP resilience enhancement strategies, which are categorized into two phases, namely pre-event reinforcement and post-event recovery, based on cascaded failure events. In the first phase, various typically used classes of pre-event reinforcement strategies were investigated, and a VPP line importance calculation method in which static network flows were considered, was used. A node importance identification method based on the contribution of neighbor nodes was modified for the VPP system. In the second phase, a timing scheme for VPP resilient recovery was proposed for the VPP system after cascade failure, and a resilience index was constructed to evaluate the performance of system network resilience with the recovery strategy. This method is convenient for managers to make rapid decisions in emergency situations and reduce the adverse effects resulting from cascade failure accidents.

Specifically, the main contributions of this paper are as follows:

(1) Although some investigators have evaluated resilience enhancement in power systems, VPP systems are yet to be considered. This study is the first on the problem of resilience enhancement of VPP systems during cascade failure events.
(2) A guiding strategy for system protection before an event is proposed from the two aspects of transmission line and components to avoid VPP system failure.
(3) A resilience measurement method was combined with a timing scheme for VPP recovery. We designed a post-disaster recovery strategy for a VPP system to enhance the resilience recovery performance of the VPP.

2. Pre-event reinforcement strategies

The pre-event reinforcement strategy is mainly used to prepare and prevent critical system component failures. The element failure rate is reduced by elevating the disaster resistance of components or lines, and this, in turn, decreases the probability of cascade failure events and the scale of system failure and improves the resilience of the VPP system. To avoid a severe network failure resulting from cascade failures, prediction analysis and preventive measures are effective elastic enhancement methods.

2.1. Line importance calculation

A VPP exhibits characteristics of an information physical fusion system, and two flow characteristics, namely information flow and energy flow, should be considered when evaluating the importance of VPP lines. Therefore, referring to a previously studied method [28], the VPP line significance is calculated with the following four steps:

(1) Communication line importance

$$LQ^{C}(e_{ij}) = \partial = \frac{\max\Phi_{e_{ij}}}{BW_{e_{ij}}} \tag{1}$$

where $\Phi_{e_{ij}}$ represents the quantity of data passing through a certain channel in a unit of time.

$$LCS^{C}(e_{ij}) = \sum_{o,d\in V_C, e^{*}_{od}\in E_C} \frac{Delay\_L_{od}}{1_N^T[Delay\_L_{od}]_{N\times N}1_N} \tag{2}$$

$$\begin{cases} \text{Delay}\_L_{od} = \gamma_{od} \times \omega_{od} \\ \omega_{od} = \dfrac{1}{\gamma_{od}} \sum\limits_{e_{ij}\in E_{od}} \text{Delay}\_e_{ij} \end{cases} \tag{3}$$

where 1_N is a column vector of N elements equal to 1,o is the VPP coordinating control center, and d is either data layer node.

(2) Power line significance.

$$LQ^{P}(e_{ij}) = 1 - \frac{\alpha_{LOSS}(e_{ij})}{\sum_{e_{ij}=1}^{E}\alpha_{LOSS}(e_{ij})} \tag{4}$$

$$LCS^{P}(e_{ij}) = \frac{P_{od}}{1_N^T[P_{od}]_{N\times N}1_N} \tag{5}$$

$$P_{od} = \frac{P_L(d)}{P(d)} A_{uod}^{-1} P_G(o) \tag{6}$$

where $A_{uod}^{-1} = [A_u^{-1}]_{od}$ is the sequential distribution matrix [29], as expressed in Eq. (7), where γ is the set of nodes supplying power directly to node$i$.

$$[A_u]_{ij} = \begin{cases} 1, i = j \\ -\dfrac{|P_{j-i}|}{P_j}, j \in \gamma \\ 0, other \end{cases} \tag{7}$$

(3) Coupling line importance

The importance of the coupled line is indicated by the sum of the share of the power of the generation node and the load node after the power flow calculation.

$$LCS_{CP}(ij) = \frac{P_{G_i}}{\sum_{i=1}^{N_G} P_{G_i}} + \frac{P_{L_i}}{\sum_{i=1}^{N_L} P_{L_i}} \tag{8}$$

(4) VPP line importance based on the optimal assignment method

A combination of hierarchical analysis [30] and the inverse entropy weighting method [31] was used to integrate the aforementioned indicators into a comprehensive assessment of line importance in the VPP. Assuming$W_1 = [w_{11}\ \ w_{21}\ \ w_{31}]^T$,$W_2 = [w_{12}\ \ w_{22}\ \ w_{32}]^T$, the optimal weighting vector is$W = \theta_1 W_1 + \theta_2 W_2$, where θ_1 and θ_2 are the optimal weighting coefficients.

2.2. Node importance calculation

Similar to line importance, the identification and protection of critical nodes enhances the ability of the VPP to resist cascade failure. Because of the specific nature of energy transfer in the VPP, the importance of each component is not only related to its nature but also influenced by the magnitude of the energy value contributed by its neighboring nodes.Focusing only on isolated nodes will lead to inaccurate network information [32]. Therefore, the existing method of calculating the node importance considering the contribution of neighboring nodes is improved according to the following steps to make it more applicable to VPP systems.

(1) Nodal efficiency:

$$NE_i = E - E_i \tag{9}$$

where E is the original network efficiency, and E_i is the efficiency of the network after removing node$i$.

(2) Nodal balance:

$$NB_i = \frac{N_{od}(i)}{\sum_{1=o<d\leqslant N} N_{od}} \tag{10}$$

where $N_{od}(i)$ represents the number of information flow and energy flow transmission paths affected by the failure of node$i$, N_{od} represents the total number of information flow and energy flow transmission paths in the network.

(3) Load importance is calculated as follows:

$$L_i^C(0) = \frac{TL \cdot k_i^\tau}{\sum_{i\in V_C} k_i^\tau} \tag{11}$$

$$TL(0) = \sum_{i\in V_P} \alpha \cdot k_i^t \tag{12}$$

$$L_i^P(0) = \beta \cdot k_i^\varphi \tag{13}$$

The node load importance is calculated as follows:

$$LI_i = \frac{L_i(0)}{\sum_{i=1}^N L_i(0)} \tag{14}$$

(4) Importance of nodes after optimal assignment is expressed as follows:

$$C_i = \omega_1 NE + \omega_2 NB + \omega_3 LI \tag{15}$$

(5) VPP node importance is detailed as follows:

$$NI_i = C \cdot H_N \tag{16}$$

$$H_N = \begin{bmatrix} 0 & a_{12}\frac{B_{21}}{\sum_{j=1}^N B_{2j}} & \cdots & a_{1N}\frac{B_{N1}}{\sum_{j=1}^N B_{Nj}} \\ a_{21}\frac{B_{12}}{\sum_{j=1}^N B_{1j}} & 0 & \cdots & \vdots \\ \vdots & \vdots & \ddots & \vdots \\ a_{N1}\frac{B_{1N}}{\sum_{j=1}^N B_{1j}} & \cdots & \cdots & 0 \end{bmatrix} \tag{17}$$

where$C = [C_1, C_2, \cdots, C_N]$,$B_{ij} = \sum_{\substack{1\leqslant l<m\leqslant N \\ (l,m)\neq(i,j)}} [N_{lm}(e_{ij})/N_{lm}]$ are the number of edges in the line connecting node i to node j, N_{lm} is the number of shortest paths between node l and node m, and $N_{lm}(e_{ij})$ is the number of these shortest paths through route e_{ij}.

3. Post-incident recovery strategy

3.1. Cascade failure process

When a component in the VPP fails, its load is redistributed to neighboring nodes in accordance with the coupling between the systems, which results in the overloading of the neighboring nodes, thereby triggering a cascade failure and causing total or local failure of the VPP. An optimal assignment model based on three types of load distribution methods was used to simulate VPP cascade failure. The influence of the importance of the nodes, performance difference, and remaining capacity on the load redistribution strategy was considered comprehensively, and a flowchart is displayed in Fig. 2.

Specifically, the cascade failure process is as follows:

(1) Initialization: The complete VPP is initialized to obtain the initial load of the nodes, and the initial load of each node is expressed as displayed in Eqs. (11–13), with the capacity set to the following equation:

$$C_i = (1+\delta)L_i \tag{18}$$

where L_i is the node load before failure.

(2) Initial failure node: Here, μ proportion of nodes to attack is randomly selected. Because of the various complexities of the services undertaken by each node in the VPP, the nodes exhibit distinct resilience characteristics to perturbations. The attack complexity of a node was measured according to the importance of the node and the probability of node failure when p is quantified.

$$p_i = 1 - NI_i \tag{19}$$

(3) Load redistribution of failed nodes: The amount of load passed from the overloaded failed node to its normal neighbor node at moment t can be expressed as follows:

$$\Delta L_{ij} = L_i \Omega_{ij} \tag{20}$$

To eliminate the effect of a single allocation method on network cascade failures, the optimal assignment method was used to obtain the final load allocation coefficients by weighting a combination of the node importance-based reallocation strategy, the neighboring node similarity allocation strategy, and the residual capacity allocation strategy, as expressed in the following equation:

$$\Omega_{ij} = \eta_1 \frac{NI_j}{\sum_{l\in\Gamma_i} NI_l} + \eta_2 \frac{|NI_i - NI_l|}{\sum_{l\in\Gamma_i} |NI_i - NI_l|} + \eta_3 \frac{C_j - L_j}{\sum_{l\in\Gamma_i}[C_l - L_l]} \tag{21}$$

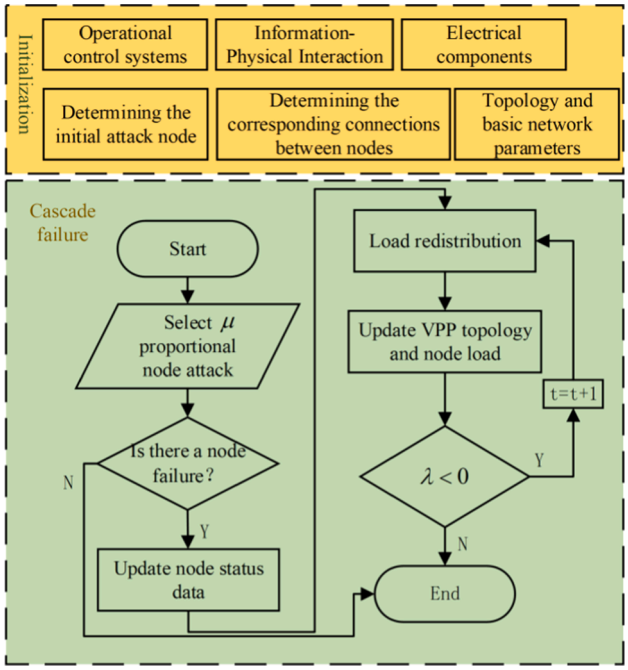

Fig. 2. Cascade failure process.

(4) Overload detection: The difference λ between the node load and the capacity after the update is calculated. If $\lambda < 0$ fails, then the node continues to work.

3.2. Recovery process

A sequential recovery scenario was considered in the VPP in which the failed node can be recovered sequentially by reestablishing the line between the node and the restored part. A flowchart of the model is displayed in Fig. 3. The edge and load of a node recovers to the initial state simultaneously, and the priority of recovery is given to the neighbors of the node because when no external control system guides limited recovery resources, repairing neighboring nodes is easier than repairing remote nodes because limited work and time is required. Most studies on coupled information-physical systems have focused on the effect of information faults on the power network. However, changes in the structure or operation of a power network considerably affects the effective operation of an information network. To recapitulate the real system, the recovery process should also satisfy the following constraints:

(1) Generator output constraints are expressed as follows:

$$\begin{aligned} P_{Gi}^{\min} \leqslant P_{Gi}^{t} \leqslant P_{Gi}^{\max} \\ Q_{Gi}^{\min} \leqslant Q_{Gi}^{t} \leqslant Q_{Gi}^{\max} \ \forall i \in \Lambda_G^t \end{aligned} \tag{22}$$

(2) Bus voltage size constraints are expressed as follows:

$$V_j^{\min} \leqslant V_j^t \leqslant V_j^{\max} \ \forall j \in \Lambda_N^t \tag{23}$$

where $V_j^{\min}$ and $V_j^{\max}$ are the minimum and maximum values of the voltage at node$j$, respectively.

(3) Transmission line capacity constraints are as follows:

$$\sum_{e_{ij} \in \Delta_{e_{ij}}^t} P_{e_{ij}}^t \leqslant P_{OLC} \tag{24}$$

where $P_{e_{ij}}^t$ is the actual active power of transmission line e_{ij} at time$t$, and P_{OLC} is the online capacity.

3.3. Resilience indicators

In existing resilience assessment methods, one or several assessment metrics are used to measure changes in system resilience, primarily from a complex network [33] or power transmission perspective [34]. However, in the VPP, transmission of energy flows in the system considerably affects system resilience. Therefore, the resilience indicator in the recovery process is defined as follows:

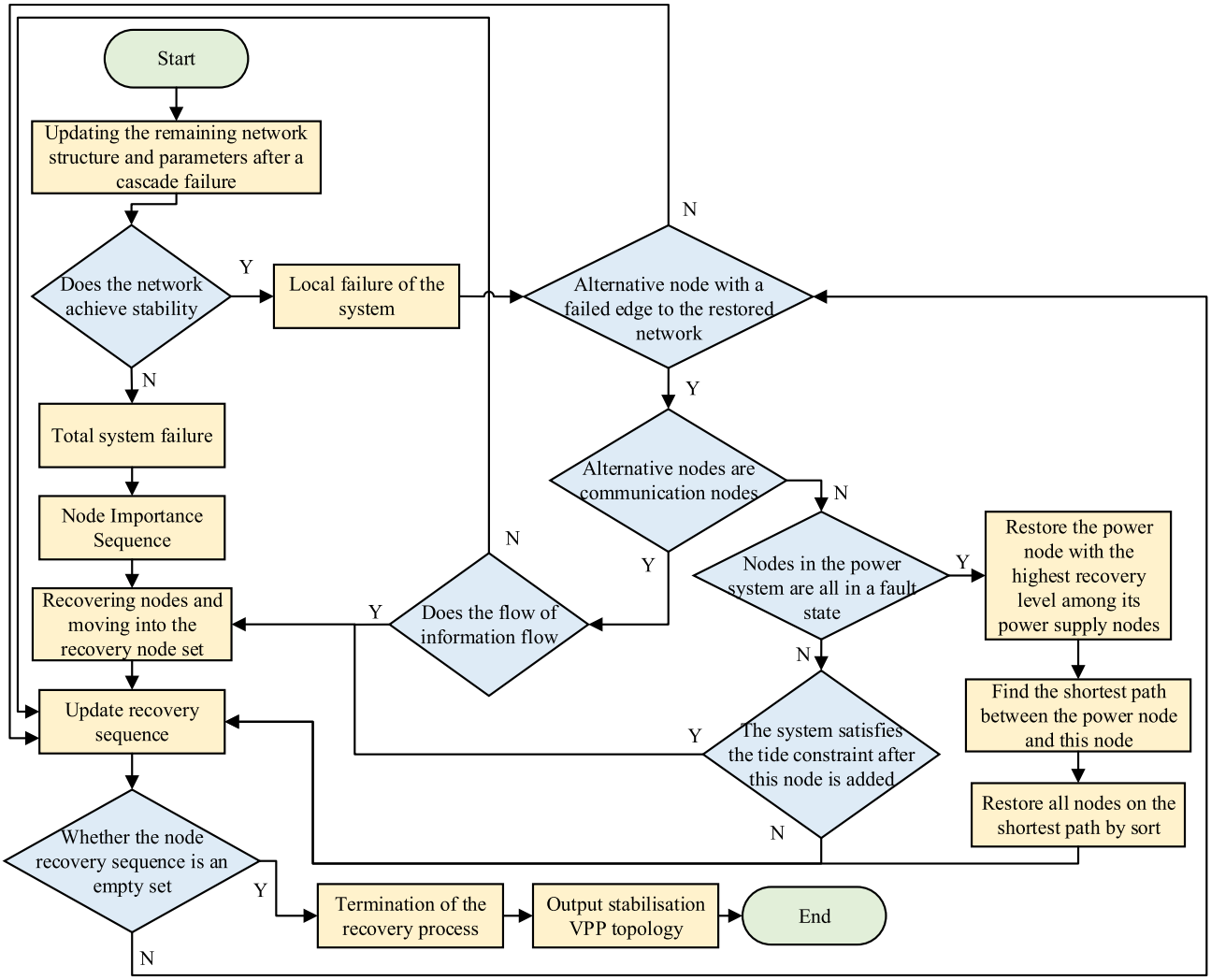

Fig. 3. VPP fault recovery process.

$$R = R(\Theta, \varpi, t) = \frac{\sum_{\varpi}\sum_{1}^{t}\Theta(t)}{(|t|\cdot|\varpi|)} \tag{25}$$

where ϖ is the system recovery size.

To comprehensively assess VPP resilience, resilience assessment indicators were constructed at the power grid and information network levels. The model has four components, namely restored power supply active power (R_{P_G}), load active power (R_{P_L}), number of information flow lines (R_{E_I}), and number of VPP system transmission lines (R_{E_V}). Next, the optimally weighted VPP system resilience index is expressed as follows:

$$R = \omega_1 R_{P_G} + \omega_2 R_{P_L} + \omega_3 R_{E_I} + \omega_4 R_{E_V} \tag{26}$$

4. Simulation validation

The IEEE30 [35] node system is used as the base power network. The VPP multi-layer network structure that was used to verify the efficacy and rationale of the proposed strategy is displayed in Fig. 4. The first layer is the coordination and control center of the VPP, which is used to track the terminal information of the VPP. The second layer is the local agent layer, which is used to process the terminal information from the lower levels and pass it to higher levels. The third layer is the energy layer, which is equipped with data acquisition equipment for each power unit. The fourth layer is the electrical layer, which consists of various electrical components. The power layer is the basic network based on the IEEE30 system topology. The first layer to the third layer is the network model of VPP operation control system under centralized-decentralized control. According to the actual characteristics of power communication network coupling of the VPP system, the communication equipment of energy layer is typically arranged in the power network, and their distribution corresponds to each other. Therefore, the network structure of the energy layer exhibits strong topological similarity with that of its corresponding power grid, and it is completely coupled to the power network in a one-to-one relationship. All components are assumed to be intact after a failure. The communication system simulation is completed using the OPNET software, and the detailed parameters of the power generation and load are presented in MATPOWER [36].

4.1. Node and line importance calculation

The calculation method of node importance considering the contribution of neighbor nodes was adopted in the study, and the extends to the VPP system. By giving priority protection to the nodes with the highest importance ranking, the cascading failure of VPP systems because of natural disasters and human factors can be avoided as much as possible. Fig. 5 reveals the node metrics and the final importance calculation results for each node. The node efficiency and balance can be used to effectively assess the importance of a node at the topological level from the perspective of information and energy flow. Additionally, load importance can be used to refine the assessment process at the level of load distribution.

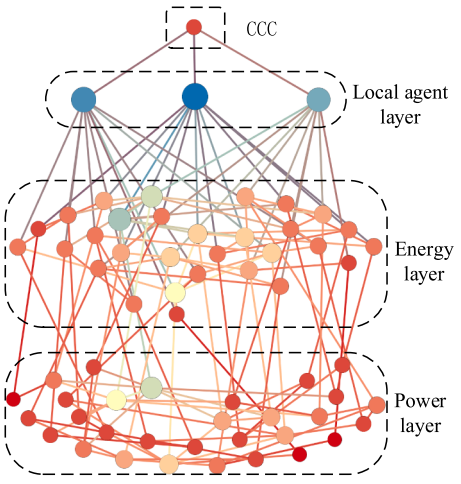

Fig. 4. Multi-layer network structure of the VPP system.

Fig. 5(e) reveals that node 1 has the highest importance because node 1 is the coordination and control center of the whole VPP system and is used for all information processing tasks. Node 60 is at the edge of the network and has fewer connected components. The active power of its load in the grid is only 1.85% of the total active power of the load; therefore, node 60 exhibits the lowest importance value after combining all the indicators. The nodes of the central layer and the local agent layer are critical because they are the "hub" of the whole network. Calculating the importance of each component in VPP can provide reference for the daily maintenance of VPP system operators.

To verify the effectiveness of this method, the following three cases are considered:

Case1: Consider only a single metric;
Case2: Consider the optimal weighted index of the target node itself;
Case3: Consider the metrics of neighbor nodes.

Fig. 6 displays the node importance curves of various cases. In Case 1, the node importance calculated by indicators with various emphases differs considerably. After the optimal weighting operation, the Case 2 curve decreases as a whole and remains the same as the curve of Cases 1, which is caused by the high weight ofNB_i. The node importance value is generally low, most of which are less than 0.3. Therefore, neighbor nodes are included in the importance evaluation category, as presented in Case 3. Because of the close relationship between the components in the VPP system, the importance of each component is improved after considering the neighbor nodes. In this evaluation method, it is not only that all types of indicators are considered and neighboring nodes participate in the evaluation system, but also that the final value is not considered to be too high or too low because of over reliance on a certain indicator.

Because of the presence of both the information flow for command data transmission and the energy flow for the power supply in the VPP line, the method for calculating the importance of the lines includes two forms of flow, namely information and energy flows. Following the steps described in Section 2.1, the importance of information transmission lines and the importance of the power transmission lines are assessed separately. The results of the calculation are displayed in Fig. 7. Fig. 7 (a–b) represents the mass fraction of the information flow and energy flow lines. The line quality represents the line utilization and the power loss on the line. The higher the line quality is, the more likely the link is a limiting link in a VPP system. The overall quality of energy flow lines is higher than that of information flow lines, which may be related to the selection of indicators. Fig. 7(c) displays the line importance of the VPP system, considering $e_{5,7}$ as an example, its energy flow line criticality is 1, but its criticality score in VPP system is 0.538. As a key component connecting the two systems, the coupling line ensures transmission and issuance of control instructions of the VPP system. The power node connected by $e_{6,36}$ has both load and generation characteristics, and its generation power and load power account for 31.81% and 11.47%, respectively, which play a critical role in the power network. Nodes 6 and 36 ranked 39th and 13th in importance, respectively, and a total of 22 pairs of network flows transmitting through $e_{6,36}$. Therefore, line $e_{6,36}$ is ranked first in importance.

The node and line importance calculation method presented in this study can be used to determine the importance of the nodes and lines in the VPP. Based on these results, the components and transmission lines in the VPP can be reinforced. The resilience of the VPP to cascading failure events is improved by implementing contingency measures before the occurrence of failure, as well as focused protection decision

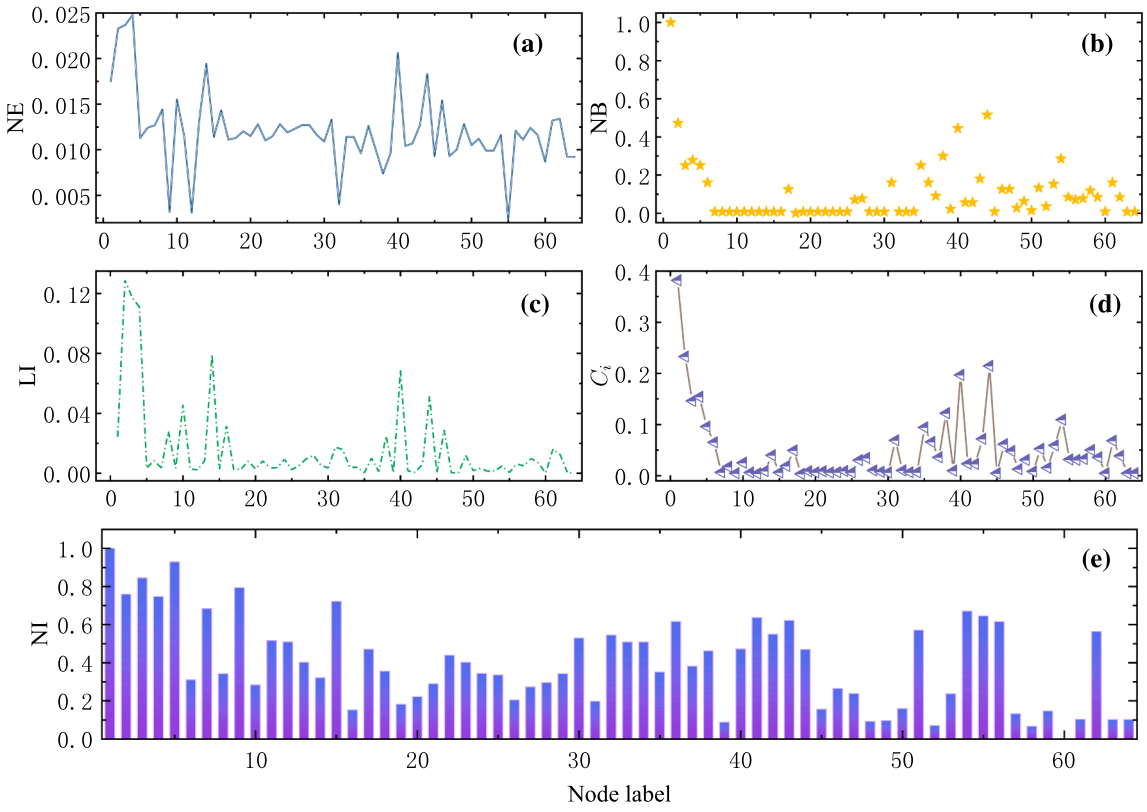

Fig. 5. Node importance (a) Nodal efficiency (b) Nodal balance (c) Load importance (d) Node importance after optimal assignment (e) Importance of VPP nodes considering the contribution of neighboring nodes.

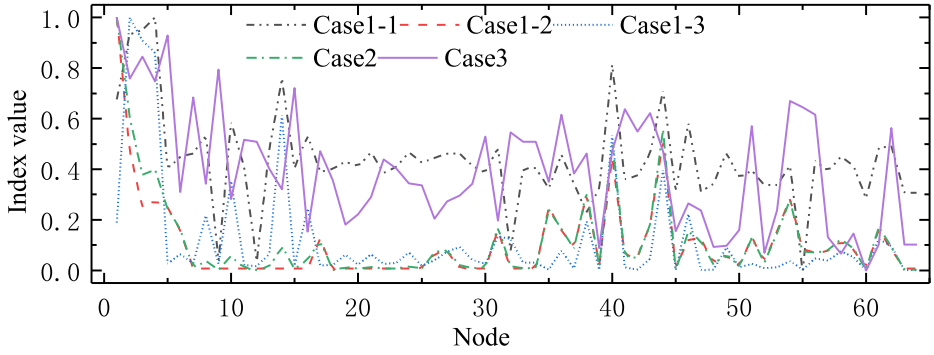

Fig. 6. Comparison of node importance in various cases.

control.

4.2. VPP cascade failure process

First, cascade failure is triggered by randomly attacking seven nodes ($\mu = 0.1$) from the VPP system, as displayed in Fig. 4. The probability of failure of the selected node can be obtained from Eq. (19). The parameters of the load redistribution process are set as follows:$\delta = 0.5, \tau = \alpha = \beta = \varphi = 1$. Fig. 8 displays the process of a cascading failure in a VPP system from the perspectives of both the network structure and the system load. The network parameters reflect to some extent the overall performance of the nodes and the network, and also relate to the cost of constructing the network. As displayed in Fig. 8(a), numerous normal nodes and edges in the network exhibit the same decaying trend. Because faults develop, more components of the system are isolated, and the number of network components increases. A brief upward trend occurred in the network diameter. When cascade failure occurs at the edge of the network, the diameter decreases, and when cascade failure occurs at intermediate nodes of information transmission, the diameter of the system as well as the average path length increases because of the growth of the transmission path. The rest of the indicators decrease slowly with the increase in cascade failure. Thus, the load redistribution approach used in this paper can slow down the cascade failure process and avoid explosive network collapse due to disasters. Fig. 8(b) displays the system load lost at each step in the development of a cascade failure event. Thus, the time period that has the most profound effect can be obtained from the cascade failure. Because of the sixth load redistribution process, the number of overloaded nodes is as high as 17, which results in the number of nodes operating normally in the network close to the number of lines. Therefore, considerable load loss during this time period. The load variation of each element in the VPP and its capacity are displayed in Fig. 8(c). In the figure, the black line indicates the capacity of each VPP element. Component failure occurs when the load at a given time exceeds the capacity of that node. For example, node 20

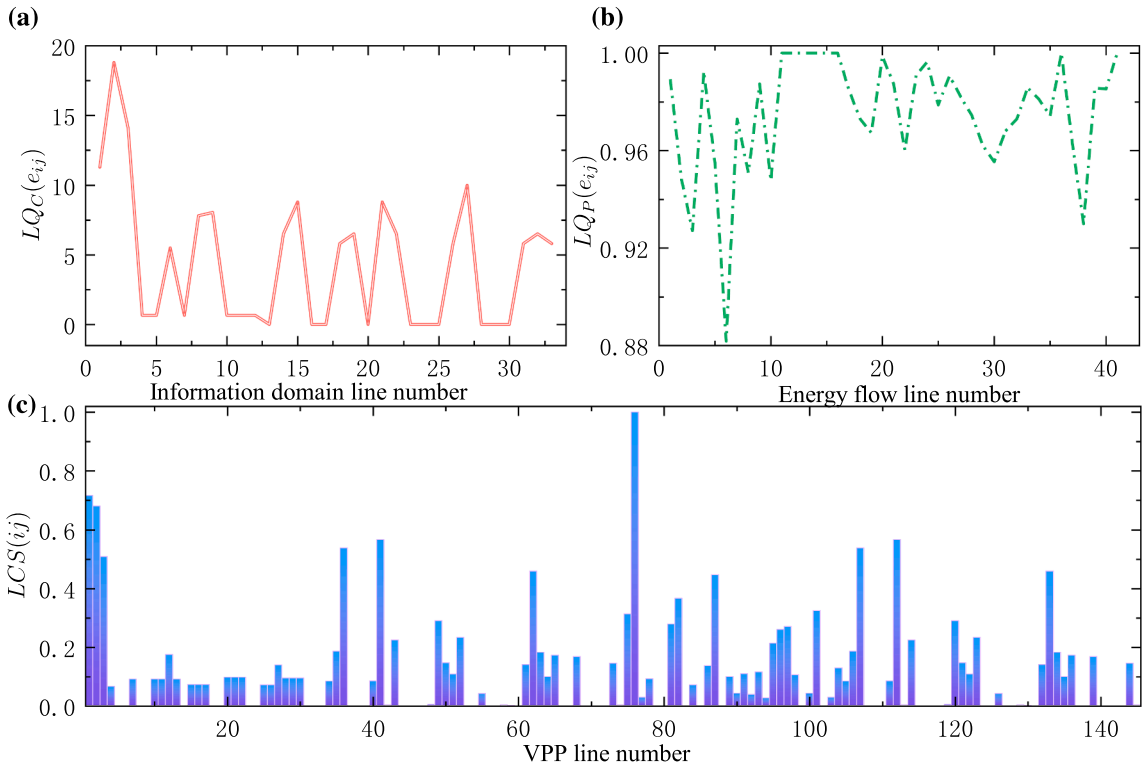

Fig. 7. Line importance (a) Information domain line quality (b) Energy flow line quality (c) VPP line importance score.

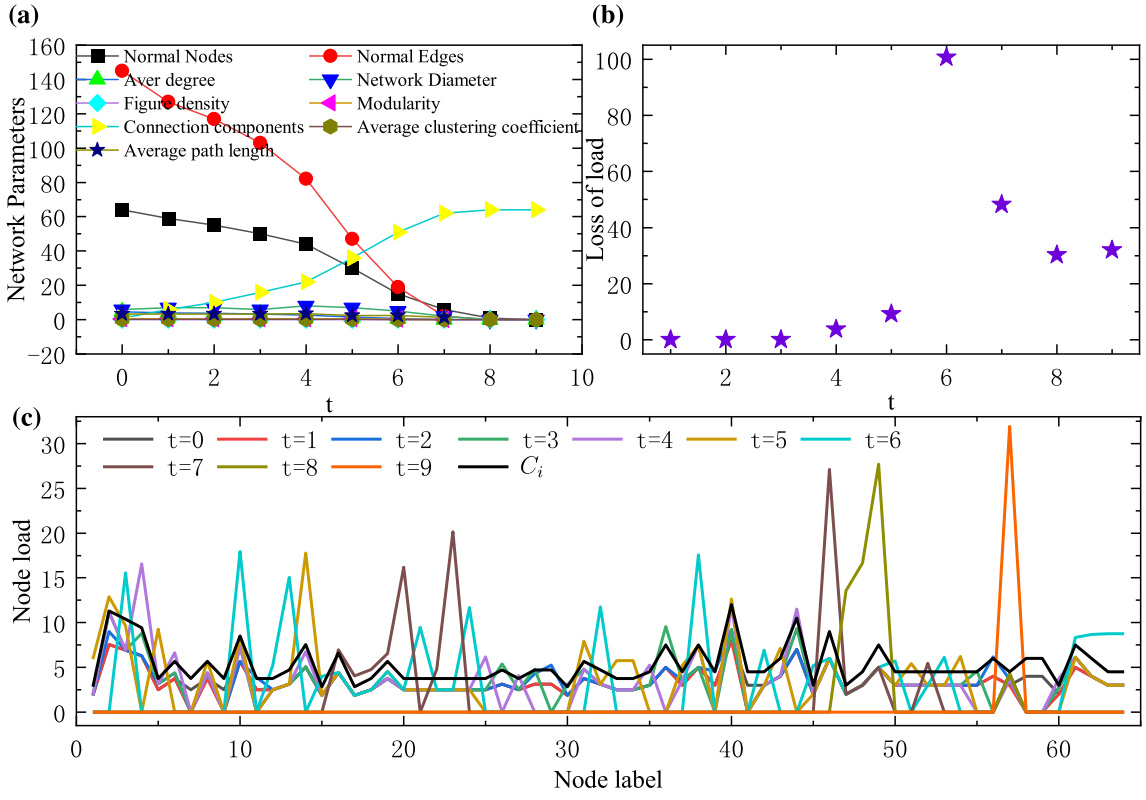

Fig. 8. Network performance variation curve during cascade failure (a) Change in network parameters per unit time step (b) Loss of load per unit time step (c) Load variation and capacity of each node.

exceeds node capacity $C_{20} = 3.78$ at $t = 5$. Therefore, the node fails and distributes its load to neighboring nodes in the manner expressed in Eq. (21).

4.3. VPP recovery process

Currently, there is limited research on timing recovery strategies,

and the recovery priority of components should be set according to node importance in the timing recovery process of VPPs. In previous studies, degree [37], betweenness [38], and load [39] have been widely used in node importance measures. Therefore, eight recovery strategies are considered based on these three types of metrics, namely, this paper's strategy (TP), a high-degree based strategy (HD), a low-degree based strategy (LD), a high-betweenness-based strategy (HB), a low-betweenness based strategy (LB), a high-load based strategy (HL), a low-load based strategy (LL), and a random strategy (RO) have been conducted.

Fig. 9 displays a comparison of the topology of the recovery network at three moments for various recovery strategies. Here, the red nodes represent the recovered VPP elements, and the black nodes represent the VPP elements that are still in fault. Fig. 9 reveals the recovery performance of this strategy is better than or equal to that of other strategies for the recovery sequence length$t = 3, 30, 60$. When $t = 60$, the unrecovered nodes in this paper are labeled 60, 58, 52, and 48, all of which are in edge positions in the VPP system. These four nodes are all load nodes whose load active power only accounts for 11.42% of the total load active power. Additionally, in the high degree–based recovery strategy, the unrecovered node 47 is the power node, and its generated active power accounts for 19.31% of the total generated active power. Although the percentage of active power of the load of the unrecovered nodes in the strategy based on a high betweenness is lower than that of this study, unrecovered nodes cause five pairs of network streams to be blocked from transmitting communication. The rest of the recovery strategies include the VPP coordination control center or agent layer nodes. In summary, the recovery strategy is more practical and reasonable than the comparison strategies.

Fig. 10(a) plots the change curve of each resilience indicator of the system before optimal weighting. A comparison of the eight curves for R_{P_L} reveals that the TP strategy does not restore as much active power to the load as the HL strategy in the middle and late stages because the fragmented location of the HL strategy's pre-repair nodes, which are not connected, and the explosive growth of the connected components when a node appears as a "threshold." A comparison of the R_{E_V} curves reveals that both the HB and TP strategies effectively restore the flow of the network flows in the VPP without considerable jumps. A comprehensive comparison reveals that the proposed repair strategy can effectively improve the overall performance of the network. Fig. 10(b) displays the resilience change curve of the VPP system for each recovery strategy. As the simulation shows, although all of the recovery strategies can restore system resilience, the best performance in the test case was observed for the recovery strategy proposed in this study. The recovery strategy based on high betweenness is second only to the strategy proposed in this paper because the larger the number of nodes is, the more "triangular" connections the node has. Therefore, the load transmitted in the network is greater. In this test case, the resilient properties increase with the length of the recovery sequence. The improved recovery of the resilience indicators indicates flexible adjustment of the generation and information transmission during the VPP redispatch, which can enhance the resilience of the VPP system to cascade failure events. However, adjustment of the parameters within the system is also limited by the constraints described in Section 3.2. Therefore, the trend of network resilience recovery flattens out as the recovery time gradually increases. Thus, the resilience enhancement strategy can effectively restore the resilience of the VPP system after cascade failure.

To intuitively detail the effectiveness of this method, the numerical comparison results of eight recovery strategies are listed in Table 1. The final elasticity index of this method is considerably improved compared with the other seven strategies. The HB strategy exhibits a high value in indicators R_{E_I} andR_{E_V}, therefore, the method ranks second. Because both R_{P_G} and R_{P_L} are related to the node load, the HL strategy exhibits considerable advantages. Table 1 reveals that the proposed method can effectively improve the flexibility of the VPP system, and the maximum improvement value can reach 18%, which can provide a reference for the daily maintenance cost of VPP administrator' and post-disaster repair.

5. Conclusion

To solve the problem of existing recovery strategy by only considering a single time period, a two-stage recovery strategy coordination and optimization framework was proposed for VPP system resilience improvement. In this method, the importance of each component in the VPP system was investigated from the perspective of system performance to detail the system recovery process over a time horizon. Considering the constructed VPP system as an example, theoretical and simulation experiments revealed that the implementation of hardening strategies for critical nodes and lines can considerably affect network resilience in terms of the network structure, energy transmission, and load. The proposed resilience enhancement strategy maximizes the resilience of the system compared with other methods in the event of a cascading failure because of an attack. This VPP resilience recovery method considering time and component importance is simple and efficient. The emergency repair plan can be rapidly formulated after the disaster to quickly recover the damaged key functions of the system. In the future, a dynamic recovery-oriented resilience enhancement strategy should be developed for VPP system dynamic resilience assessment and in-event recovery strategy to provide a theoretical basis for

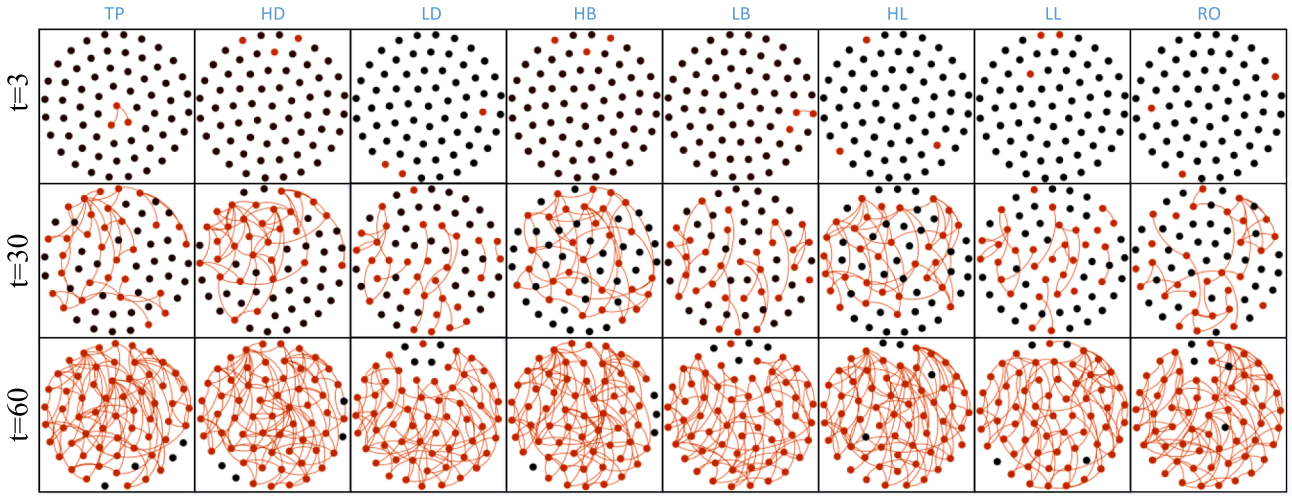

Fig. 9. Network topology at $t = 3$, $t = 30$, and $t = 60$ for various recovery strategies during VPP system recovery.

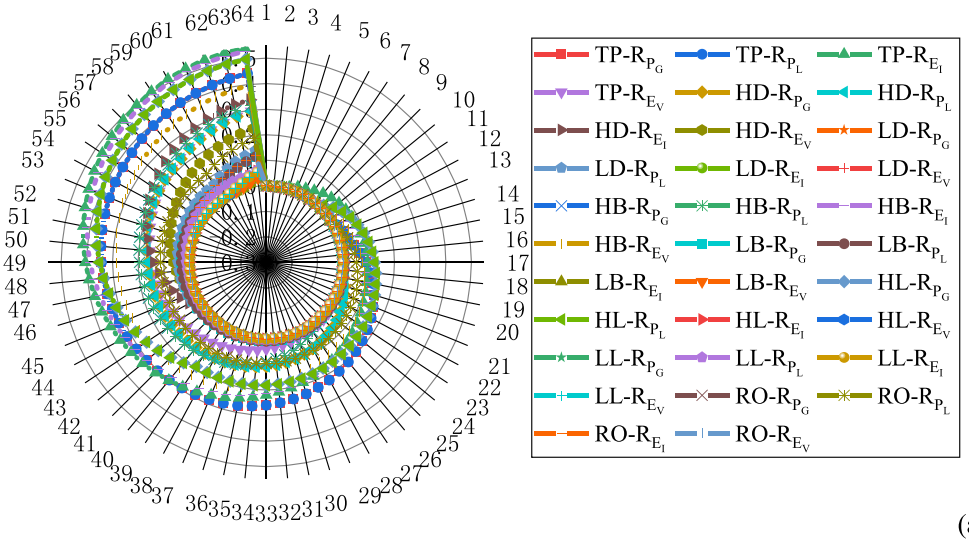

(a)

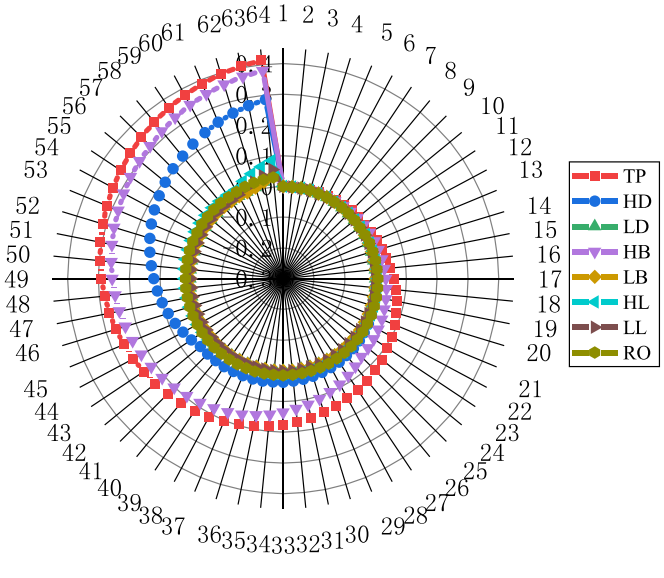

(b)

Fig. 10. Resilience indicators during recovery (a) Curve for indicator R_{P_G}, R_{P_L}, R_{E_I}, and R_{E_V} (b) Curve for indicator R.

Table 1
Comparison of network average resilience indexes.

	TP	HD	LD	HB	LB	HL	LL	RO
R_{P_G}	**0.22**	0.1	0.03	0.1	0.02	**0.22**	0.01	0.08
R_{P_L}	**0.22**	0.1	0.03	0.1	0.02	**0.22**	0.01	0.08
R_{E_I}	**0.24**	0.07	0.00	**0.23**	0.00	0.00	0.00	0.01
R_{E_V}	0.08	0.04	0.00	**0.18**	0.00	0.00	0.00	0.01
R	**0.18**	0.07	0.00	**0.15**	0.00	0.02	0.00	0.01

responding to large-scale DER grid connections in the future and improve the operational efficiency of power systems.

CRediT authorship contribution statement

Yue Meng: Conceptualization, Methodology, Software, Investigation, Formal analysis, Writing – original draft. **Hongli Zhang:** Conceptualization, Funding acquisition, Resources, Supervision.

Declaration of Competing Interest

The authors declare that they have no known competing financial interests or personal relationships that could have appeared to influence the work reported in this paper.

Acknowledgement

The authors gratefully acknowledge the financial support from the National Natural Science Foundation of China (51967019, 52065064) ; the Xinjiang Uygur Autonomous Region Tianshan Youth Plan Project (2020Q066) ..

References

[1] Guangming Online. Carbon peaking, carbon neutrality, these international lessons can be learned. https://baijiahao.baidu. com/s?id=1698334555166347129&wfr=spider&for=pc, April 29, 2021.
[2] Yu S, et al. Uncertainties of virtual power plant: Problems and countermeasures. Appl Energy 2019;239:454–70.
[3] He Sizhe, et al. Detection Method for Tolerable False Data Injection Attack Based on Deep Learning Framework. 2020 Chinese Automation Congress (CAC). IEEE; 2020.

[4] Gardiner Joseph, Awais Rashid. Technical Report: Gone in 20 Seconds–Overview of a Password Vulnerability in Siemens HMIs. arXiv preprint arXiv:2009.03961 (2020).
[5] Bie Zhaohong, Lin Chaofan, Li Gengfeng, et al. Development and Prospect of Resilient Power System in the Context of Energy Transition. Proceedings of the CSEE 2020; 40(09): 2735-2745.
[6] Elmqvist T, et al. Sustainability and resilience for transformation in the urban century. Nat Sustainability 2019;2(4):267–73.
[7] Meuwissen MPM, et al. A framework to assess the resilience of farming systems. Agricultural Systems 2019;176:102656.
[8] Pettit TJ, Croxton KL, Fiksel J. The evolution of resilience in supply chain management: a retrospective on ensuring supply chain resilience. J Bus Logist 2019;40(1):56–65.
[9] Panteli Mathaios, et al. Power systems resilience assessment: Hardening and smart operational enhancement strategies. Proceedings of the IEEE 105.7 (2017): 1202-1213.
[10] Jufri FH, Widiputra V, Jung J. State-of-the-art review on power grid resilience to extreme weather events: Definitions, frameworks, quantitative assessment methodologies, and enhancement strategies. Appl Energy 2019;239:1049–65.
[11] Wang Y, et al. Evaluation of economic benefits of virtual power plant between demand and plant sides based on cooperative game theory. Energ Conver Manage 2021;238:114180.
[12] Tari AN, Sepasian MS, Kenari MT. Resilience assessment and improvement of distribution networks against extreme weather events. Int J Electr Power Energy Syst 2021;125:106414.
[13] Gilani MA, Kazemi Aa, Ghasemi M. Distribution system resilience enhancement by microgrid formation considering distributed energy resources. Energy 2020;191:116442.
[14] Liu J, Yixin Yu, Qin C. Unified two-stage reconfiguration method for resilience enhancement of distribution systems. IET Gener Transm Distrib 2019;13(9):1734–45.
[15] Hussain A, Bui V-H, Kim H-M. Microgrids as a resilience resource and strategies used by microgrids for enhancing resilience. Appl Energy 2019;240:56–72.
[16] Hemmati R, Mehrjerdi H, Nosratabadi SM. Resilience-oriented adaptable microgrid formation in integrated electricity-gas system with deployment of multiple energy hubs. Sustain Cities Soc 2021;71:102946.
[17] Nosratabadi SM, Hooshmand R-A. Stochastic electrical energy management of industrial Virtual Power Plant considering time-based and incentive-based Demand Response programs option in contingency condition. Int J Emerg Electr Power Syst 2020;21:2.
[18] Clegg S, Mancarella P. Integrated electricity-heat-gas modelling and assessment, with applications to the Great Britain system. Part II: Transmission network analysis and low carbon technology and resilience case studies. Energy 2019;184:191–203.
[19] Goldbeck N, Angeloudis P, Ochieng WY. Resilience assessment for interdependent urban infrastructure systems using dynamic network flow models. Reliab Eng Syst Saf 2019;188:62–79.
[20] Shao C, et al. Integrated planning of electricity and natural gas transportation systems for enhancing the power grid resilience. IEEE Trans Power Syst 2017;32(6):4418–29.
[21] Marqusee Jeffrey, Donald Jenket Don II. Reliability of emergency and standby diesel generators: Impact on energy resiliency solutions. Appl Energy 2020; 268:114918.
[22] Asyraf MRM, et al. Potential Application of Green Composites for Cross Arm Component in Transmission Tower: A Brief Review. Int J Polym Sci 2020;2020.
[23] Pourakbari-Kasmaei M, Mahmood F, Lehtonen M. Optimized Protection of Pole-Mounted Distribution Transformers against Direct Lightning Strikes. Energies 2020;13(17):4372.
[24] Correa-Tamayo JS, Arias-Londoño A, Granada-Echeverri M. Optimal management of vegetation maintenance and the associated costs of its implementation in overhead power distribution systems. TecnoLógicas 2019;22(45):93–109.
[25] Hu Y-S, Zhu C-L. Credit Evaluation Model of Road Transportation Enterprises Based on the Combination Weighting Method. Math Probl Eng 2021;2021.
[26] Liu R, Mou X, Liu H-C. New Model for Occupational Health and Safety Risk Assessment based on Combination Weighting and Uncertain Linguistic Information. IISE Trans Occup Ergonomics Human Factors 2021:1–21.
[27] Wang J, et al. Synthetic evaluation of steady-state power quality based on combination weighting and principal component projection method. CSEE J Power Energy Syst 2017;3(2):160–6.
[28] Hamedmoghadam H, et al. Percolation of heterogeneous flows uncovers the bottlenecks of infrastructure networks. Nat Commun 2021;12(1):1–10.
[29] Bialek J. Tracing the flow of electricity. IEE Proceedings-Generation, Transmission and Distribution 1996;143(4):313–20.
[30] Saaty TL. How to make a decision: the analytic hierarchy process. Eur J Oper Res 1990;48(1):9–26.
[31] Zhang H, et al. Smart grid evaluation based on anti-entropy weight method. Power Syst Protect Control 2012;40(11):24–9.
[32] Wang Yun-ming, et al. Cascading failure model for command and control networks based on an m-order adjacency matrix. Mobile Information Systems 2018.
[33] Li Y, et al. Exploiting network topology optimization and demand side management to improve bulk power system resilience under windstorms. Electr Pow Syst Res 2019;171:127–40.
[34] Tang Wenhu, Yang Yihao, Li Yajing, et al. Investigation on Resilience Assessment and Enhancement for Power Transmission Systems Under Extreme Meteorological Disasters. Proceedings of the CSEE 2020; 40(07): 2244-2254+2403.
[35] Alsac O, Stott B. Optimal load flow with steady-state security[J]. IEEE Trans Power Syst 1974;3:745–51.
[36] Zimmerman, Ray D, Carlos E. Murillo-Sánchez, Deqiang Gan. "Matpower." PSERC. [Online]. Software Available at: http://www. pserc. cornell. edu/matpower; 1997.
[37] Wang Z, Scaglione A, Thomas RJ. The node degree distribution in power grid and its topology robustness under random and selective node removals. 2010 IEEE International Conference on Communications Workshops. IEEE; 2010.
[38] Wang K, et al. An electrical betweenness approach for vulnerability assessment of power grids considering the capacity of generators and load. Physica A 2011;390(23-24):4692–701.
[39] Chaoqi Fu, et al. Multi-node attack strategy of complex networks due to cascading breakdown. Chaos Solitons Fractals 2018;106:61–6.